Fabrication and Properties of Fullerodendron Thin Films

Chisato Hirano,[†] Toyoko Imae,*[,†,‡] Shohoko Fujima,[§] Yasushi Yanagimoto,[§] and Yutaka Takaguchi[§]

Graduate School of Science and Research Center for Materials Science, Nagoya University, Chikusa, Nagoya 464-8602, Japan, and Graduate School of Natural Science and Technology, Okayama University, Tsushima, Okayama 700-8530, Japan

Received July 22, 2004. In Final Form: October 21, 2004

Thin films of fullerodendron (C_{60}(G*n*-COOMe) (n = 0.5, 1.5, 2.5)), which was synthesized from fullerene and anthracenyl poly(amido amine) dendron with methyl ester terminals and different generations (G), were fabricated by the Langmuir−Blodgett (LB) and adsorption techniques. It was characterized by X-ray reflectometry that the LB films possessed well-ordered structure, although the adsorption method led to random orientation of molecules. As to C_{60}(G0.5-COOMe) and C_{60}(G1.5-COOMe), the LB films took a four-layer structure consisting of a double layer of molecules, and fullerene moieties exist in the interior of the LB films. On the other hand, C_{60}(G2.5-COOMe) led to a two-layer structure in which the fullerene moieties were at the air side and the dendron moieties were at the substrate side. With increasing generation of dendron, the monolayer formation ability at the air/water interface as amphiphilic molecule strengthens and the amphiphilic property becomes superior to the fullerene−fullerene attractive interaction that prevents the monolayer formation. Furthermore, in the case of C_{60}(G0.5-COOMe) and C_{60}(G1.5-COOMe), the reduction peak in cyclic voltammetry of the LB film remained even after UV light irradiation. On the contrary, the peak of the C_{60}(G2.5-COOMe) LB film disappeared, indicating that molecular arrangement in the films affects electrochemical properties.

Introduction

Fullerenes and their derivatives are paid increasing attention and have been widely studied on construction of supramolecular assemblies and nanostructured devices.[1−8] Particularly, investigations on structurally ordered thin films of organofullerenes are important, since such films reveal the electrochemical and photoelectrochemical properties[9−12] and might be used for fabrication of valuable surface layers for microsensor or optoelectronic devices. To achieve fabrication of such films, binding dendron to fullerene is useful because of the highly dense and functional terminal groups of dendron.

The widely adopted approaches to prepare structurally ordered thin films of fullerenes and their derivatives are the self-assembled monolayer (SAM)[12−16] and Langmuir−Blodgett (LB)[10,17−25] techniques. The formation of fullerene-derivative-modified SAMs has been achieved through the junction moiety of carboxyl derivative,[16] organosilane,[13] OsO_4,[14] or organosulfur.[12,15] On the other hand, the LB technique, the method that fabricates Langmuir films at the air/water interface and subsequently transfers those films onto a solid substrate, also allows controlling the structure of the films at a molecular level. Fullerene derivatives were functionalized by hydrophilic additives, such as poly(ethylene glycol),[10,17,21] polyhydroxylate,[22] crown ether,[20] and oligopeptide.[24] Furthermore, the fullerene derivative, in which fullerene was incorporated into the branched moiety of dendron, was investigated as

* Corresponding author. Address: Research Center for Materials Science, Nagoya University, Chikusa, Nagoya 464−8602, Japan. Tel: +81-52-789-5911. Fax: +81-52-789-5912. E-mail: imae@nano.chem.nagoya-u.ac.jp.

† Graduate School of Science, Nagoya University.

‡ Research Center for Materials Science, Nagoya University.

§ Graduate School of Natural Science and Technology, Okayama University.

(1) Mirkin, C. A.; Caldwell, W. B. *Tetrahedron* **1996**, *52*, 5113.
(2) Jenekhe, S. A.; Chen, X. L. *Science* **1998**, *279*, 1903.
(3) Cassell, A. M.; Asplund, C. L.; Tour, J. M. *Angew. Chem., Int. Ed.* **1999**, *38*, 2403.
(4) Sano, M.; Oishi, K.; Ishi-i, T.; Shinkai, S. *Langmuir* **2000**, *16*, 3773.
(5) Brettreich, M.; Burghardt, S.; Böttcher, C.; Bayerl, T.; Bayerl, S.; Hirsch, A. *Angew. Chem., Int. Ed.* **2000**, *39*, 1845.
(6) Zhou, S.; Burger, C.; Chu, B.; Sawamura, M.; Nagahama, N.; Toganoh, M.; Hackler, U. E.; Isobe, H.; Nakamura, E. *Science* **2001**, *291*, 1944.
(7) Georgakilas, V.; Pellarini, F.; Prato, M.; Guldi, D. M.; Melle-Franco, M.; Zerbetto, F. *Proc. Natl. Acad. Sci. U.S.A.* **2002**, *99*, 5075.
(8) Nakanishi, T.; Morita, M.; Murakami, H.; Sagara, T.; Nakashima, N. *Chem.−Eur. J.* **2002**, *8*, 1641.
(9) Nakashima, N.; Tokunaga, T.; Nonaka, Y.; Nakanishi, T.; Murakami, H.; Sagara, T. *Angew. Chem., Int. Ed.* **1998**, *37*, 2671.
(10) Carano, M.; Ceroni, P.; Paolucci, F.; Roffia, S.; Ros, T. D.; Prato, M.; Sluch, M. I.; Pearson, C.; Petty, M. C.; Bryce, M. R. *J. Mater. Chem.* **2000**, *10*, 269.
(11) Nakashima, N.; Ishii, T.; Shirakusa, M.; Nakanishi, T.; Murakami, H.; Sagara, T. *Chem.−Eur. J.* **2001**, *7*, 1766.
(12) Yamada, H.; Imahori, H.; Fukuzumi, S. *J. Mater. Chem.* **2002**, *12*, 2034.
(13) Chen, K.; Caldwell, W. B.; Mirkin, C. A. *J. Am. Chem. Soc.* **1993**, *115*, 1193.
(14) Chupa, J. A.; Xu, S.; Fischetti, R. F.; Strongin, R. M.; McCauley, J. P.; Smith, A. B.; Blasie, J. K.; Peticolas, L. J.; Bean, J. C. *J. Am. Chem. Soc.* **1993**, *115*, 4383.
(15) Kitajima, N.; Komatsuzaki, H.; Hikichi, S.; Osawa, M.; Morooka, Y. *J. Am. Chem. Soc.* **1994**, *116*, 11596.
(16) Wei, T.-X.; Zhai, J.; Ge, J.-H.; Gan, L.-B.; Huang, C.-H.; Luo, G.-B.; Ying, L.-M.; Liu, T.-T.; Zhao, X.-S. *Appl. Surf. Sci.* **1999**, *151*, 153.
(17) Hawker, C. J.; Saville, P. M.; White, J. W. *J. Org. Chem.* **1994**, *59*, 3503.
(18) Nakanishi, T.; Matsuoka, H.; Nakashima, N. *Chem. Lett.* **1999**, 1219.
(19) Felder, D.; Gallani, J.-L.; Guillon, D.; Heinrich, B.; Nicoud, J.-F.; Nierengarten, J.-F. *Angew. Chem., Int. Ed.* **2000**, *39*, 201.
(20) Ge, Z.; Li, Y.; Du, C.; Wang, S.; Zhu, D. *Thin Solid Films* **2000**, *368*, 147.
(21) Giovanelli, L.; Lay, G. L. *Appl. Surf. Sci.* **2000**, *162−163*, 513.
(22) Liu, W.-J.; Jeng, U.; Lin, T.-L.; Lai, S.-H.; Shih, M. C.; Tsao, C.-S.; Wang, L. Y.; Chiang, L. Y.; Sung, L. P. *Physica B* **2000**, *283*, 49.
(23) Nierengarten, J.-F.; Eckert, J.-F.; Rio, Y.; Carreon, M. der P.; Gallani, J.-L.; Guillon, D. *J. Am. Chem. Soc.* **2001**, *123*, 9743.
(24) Tundo, P.; Perosa, A.; Selva, M.; Valli, L.; Giannini, C. *Colloids Surf., A* **2001**, *190*, 295.
(25) Felder, D.; Nava, M. G.; Carreón, M. der P.; Eckert, J.-F.; Luccisano, M.; Schall, C.; Masson, P.; Gallani, J.-L.; Heinrich, B.; Guillon, D.; Nierengarten, J.-F. *Helv. Chim. Acta* **2002**, *85*, 288.

10.1021/la048161u CCC: $30.25
Published on Web 12/02/2004

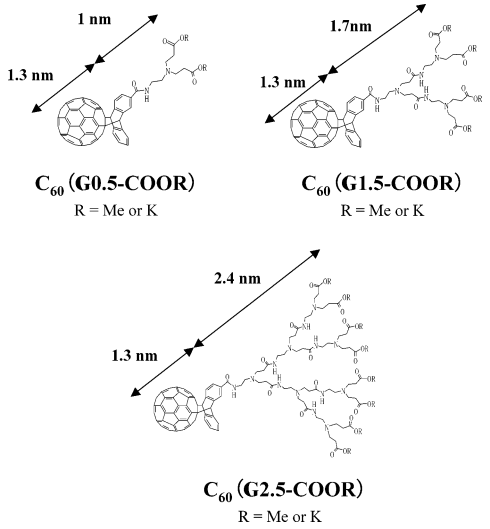

Figure 1. Chemical structures of C_{60}(G*n*-COOR).

a LB-film-constituting material.[19,23,25] However, the construction of highly ordered thin films from dendron-including fullerene derivatives is still challenging investigations.

In the present study, we report the fabrication of LB films and adsorption films of fullerene-functionalized dendrons, fullerodendrons. We expect that amphiphilicity of fullerodendrons preferably acts on the molecular arrangement, and the two-dimensional arrangement of fullerene is selectively formed by the interfullerene interaction. Molecular arrangement within the fabricated thin films is investigated by X-ray reflectometry (XR), which is one of powerful tools for the analysis of film structure. Additionally, the electrochemical properties of these films are examined with cyclic voltammetry (CV), which is sensitive to the change of electrochemical properties. Then the influence of fabrication methods, dendron generations, and terminal groups on the intrinsic electrochemical properties of fullerene is compared and discussed. For this purpose, fullerodendrons were synthesized from fullerene and anthracenyl poly(amido amine) dendron. In the fullerodendrons, fullerene is located in a focal point of a dendron and behaves as a hydrophobic moiety. The construction of ordered fullerene films and the breakthrough of intrinsic electrochemical properties by the fabrication of fullerene films are the first step to the valuable application of fullerodendron.

Experimental Section

Chemicals. According to the previously reported method,[26] fullerodendrons (C_{60}(G*n*-COOMe) (n = 0.5, 1.5, 2.5) and C_{60}(G*n*-COOK) (n = 0.5, 1.5, 2.5)) (Figure 1) were synthesized by Diels−Alder reaction of C_{60} with anthracenyl poly(amido amine) dendrons, which have various generations (G*n*) and methyl ester or potassium carboxylate terminal groups. (Fullerodendrons were previously called poly(amido amine) fullerodendrimers.) Chloroform, arachidic acid, and tetrabutylammonium chloride (TBAC) were purchased from Wako Pure Chemical Industries Co. Ltd. All chemicals were used as received without further purification. Ultrapure (Milli-Q) water (Millipore Co., 18.3 MΩ) was used throughout the experiment.

LB Films of C_{60}(G*n*-COOMe). The preparation of LB films was performed with an LB film deposition apparatus (Nippon Laser & Electronics Laboratory). A chloroform solution of C_{60}(G*n*-COOMe) (100 μM) was carefully spread by a microsyringe on the water subphase at 25 ± 0.5 °C. The solvent was allowed to evaporate for 20 min, the floating film was compressed at a rate of 10 mm min^{-1}, and the surface pressure−area (π−A) isotherm was recorded. The Langmuir films under a constant surface pressure of 20 mN m^{-1} were transferred from the air/water interface onto a silicon wafer (for XR), highly ordered pyrolytic graphite (HOPG) (for cyclic voltammetry), or a Au substrate (for infrared reflection−absorption (IR-RA) spectroscopy) by vertical dipping mode at a rate of 3 mm min^{-1}. The HOPG substrate was modified by arachidic acid LB (X-type) film. All the LB films were dried overnight in vacuo. The light irradiation was carried out on a UV irradiation light source (EX-250, Hoya-Schott Co.).

Adsorption Films of C_{60}(G*n*-COOR). Adsorption films were prepared as follows: The silicon wafers were immersed at room temperature for 5 or 24 h into chloroform solutions of C_{60}(G*n*-COOMe) or aqueous solutions of C_{60}(G*n*-COOK), respectively, at a concentration of 0.2 mM. The wafers were rinsed with solvent and dried overnight in vacuo.

Apparatus. XR measurements were performed with a Rigaku RINT 2500 X-ray reflectometer using a Cu Kα X-ray source (200 mA/40 kV) monochromized by a multilayered mirror. The sample stage was adjusted by a goniometer. The divergence slit and receiving slit were 0.05 and 0.1 cm, reflectively. Data were

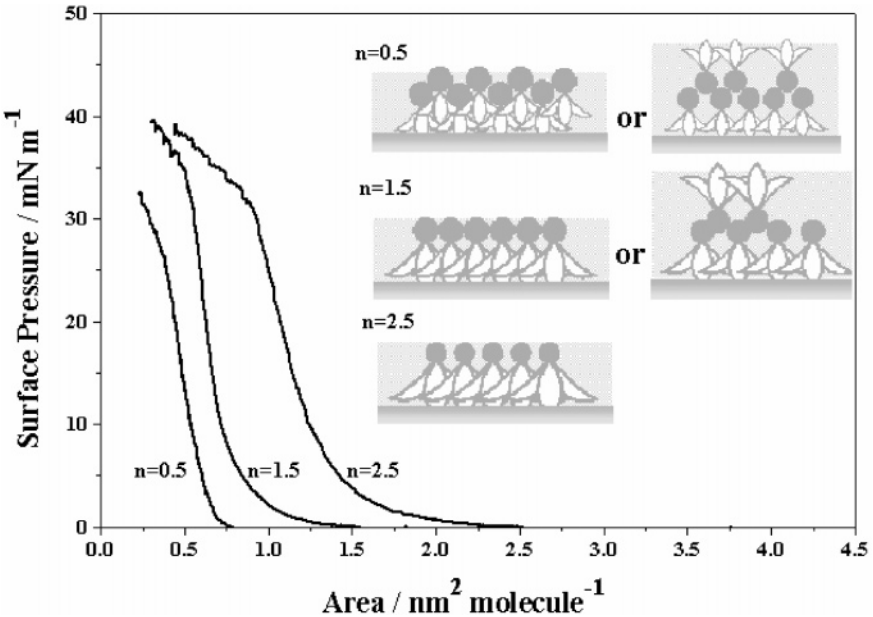

Figure 2. π−A isotherms of C_{60}(G*n*-COOMe) (n = 0.5, 1.5, 2.5) on a water subphase and schematic representation of estimated molecular arrangements.

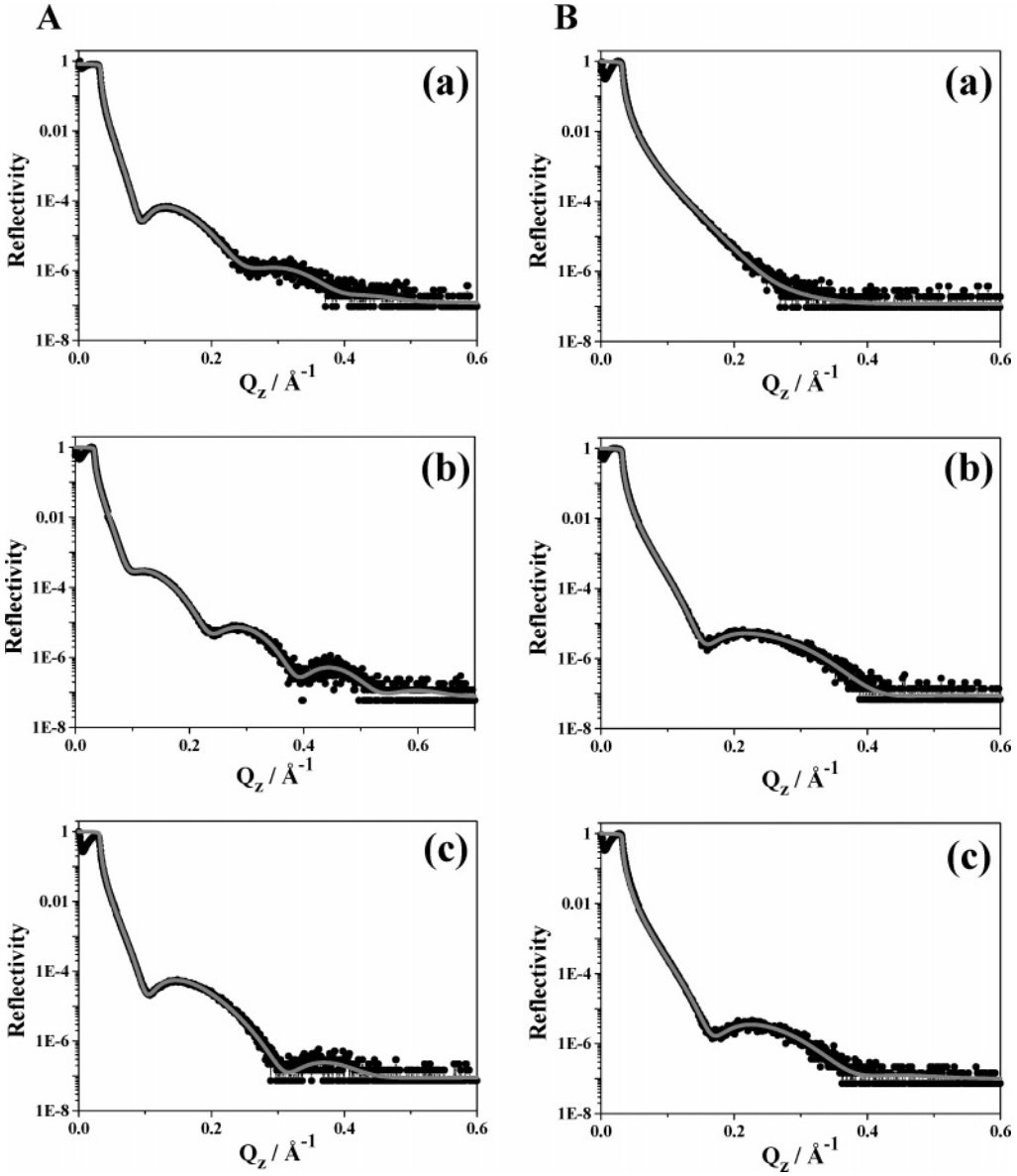

Figure 3. XR curves of (A) LB films and (B) adsorption films of C_{60}(Gn-COOMe) (n = 0.5, 1.5, 2.5) at the air/silicon interface. The closed circles are experimental data, and the solid lines are the optimum fitting curves. (a) C_{60}(G0.5-COOMe); (b) C_{60}(G1.5-COOMe); (c) C_{60}(G2.5-COOMe).

collected at 0.04° min^{-1} scan rate and with a 0.001° angle step. The XR curves were analyzed by a Fresnel equation,[27]

$$\frac{R(Q_z)}{R_F(Q_z)} = \left|\frac{1}{\rho_{sub}}\int_{-\infty}^{\infty}\frac{d\rho(z)}{dz}\exp(iQ_z z)\,dz\right|^2 \quad (1)$$

where $R(Q_z)$ and $R_F(Q_z)$ are the reflectivity and the Fresnel reflectivity ($R_F \sim Q_z^{-4}$), respectively, at a scattering vector component Q_z at the direction (=z axis) normal to the substrate surface. $Q_z = 4\pi \sin\theta/\lambda$, where θ is the incident angle, and λ is the wavelength (=0.154 nm). $\rho(z)$ means the averaged electron density of the layer at the distance z. ρ_{sub} is the electron density of the substrate. Fullerodendron consists of fullerene and dendron moieties. Then two moieties were counted as different layers, if necessary. A silicon oxide layer is formed on the surface of a silicon substrate, and both layers were included in the computer analysis. The XR curves were fitted by the least-squares method from initial values, and the optimum structure parameters (layer thickness, density contrast, and interfacial roughness) were obtained. The optimum parameters of the silicon oxide layer were commonly 2.44 ± 0.15 g cm^{-3}, 2.35 ± 0.54 nm, and 0.55 ± 0.09 nm for density, layer thickness, and roughness, respectively.

Cyclic voltammetry was performed in a three-electrode cell on a computerized electrochemical measurement system (HZ-3000, Hokuto Denko Co.). A saturated calomel electrode (SCE) and a platinum wire were used as the reference and counter electrodes, respectively. The working electrode was HOPG, which was modified with arachidic acid LB film and then C_{60}(Gn-COOMe) LB film. The supporting electrolyte used was 0.5 M TBAC in water, which was degassed by nitrogen bubbling.

IR spectra were recorded on a Bio-Rad FTS 575C FT-IR spectrometer equipped with a cryogenic mercury cadmium telluride (MCT) detector and a Harrick reflectance attachment (incidence angle, 75°). The IR spectra were collected with 1024 scans at 4 cm^{-1} resolution. UV−visible absorption spectra were measured with a Shimadzu UV-2200 spectrometer. The specimen was prepared by spreading a small drop of C_{60}(G2.5-COOMe) chloroform solution on a quartz substrate and drying.

Results and Discussion

Molecular Arrangements in C_{60}(Gn-COOMe) Langmuir Films. Figure 2 shows the π−A isotherms of

(26) Takaguchi, Y.; Sako, Y.; Yanagimoto, Y.; Tsuboi, S.; Motoyoshiya, J.; Aoyama, H.; Wakahara, T.; Akasaka, T. *Tetrahedron Lett.* **2003**, *44*, 5777.

(27) van der Lee, A. *Solid State Sci.* **2000**, *2*, 257.

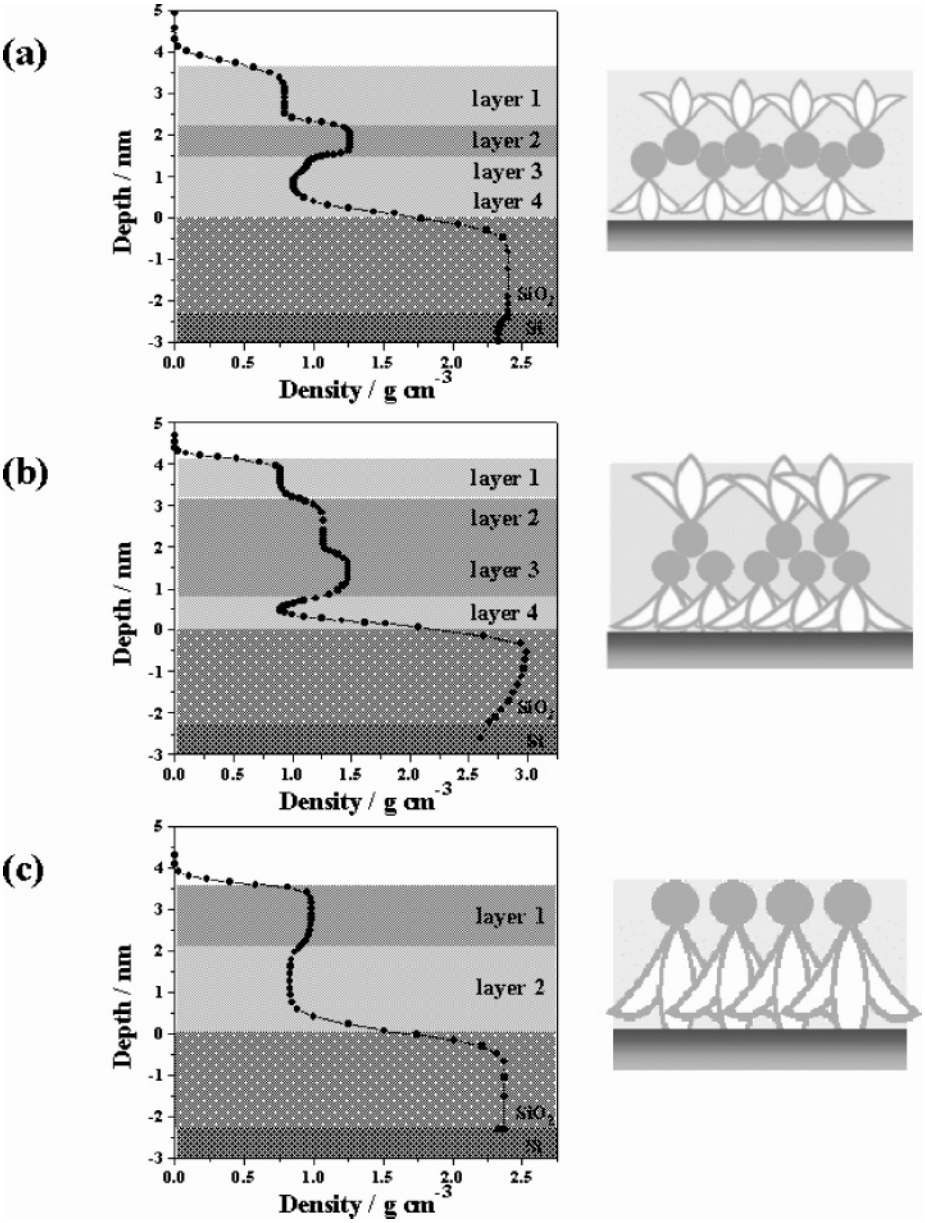

Figure 4. Depth profile of LB films of C_{60}(G*n*-COOMe) (n = 0.5, 1.5, 2.5) and schematic illustration of molecular arrangements at the air/silicon interface. (a) C_{60}(G0.5-COOMe); (b) C_{60}(G1.5-COOMe); (c) C_{60}(G2.5-COOMe).

Table 1. Structural Parameters for the LB and Adsorption Films of C_{60}(G*n*-COOR)

sample				density/g cm^{-3}	layer thickness/nm	(total thickness/nm)	roughness/nm
LB film	C_{60}(G*n*-COOMe)	n = 0.5	layer 1	0.79	1.45	(3.7)	0.43
			layer 2	1.26	0.82		0.20
			layer 3	0.96	0.41		0.16
			layer 4	0.85	1.01		0.22
		n = 1.5	layer 1	0.90	1.00	(4.0)	0.20
			layer 2	1.26	1.30		0.29
			layer 3	1.47	1.15		0.17
			layer 4	0.64	0.56		0.45
		n = 2.5	layer 1	0.98	1.55	(3.6)	0.27
			layer 2	0.83	2.07		0.41
adsorption film	C_{60}(G*n*-COOMe)	n = 0.5		1.33	0.91		0.55
		n = 1.5		0.88	2.06		0.33
		n = 2.5		1.62	2.26		0.37
adsorption film	C_{60}(G*n*-COOK)	n = 2.5	layer 1	0.7	1.87	(4.6)	0.42
			layer 2	1.43	0.75		0.51
			layer 3	0.95	1.77		0.21

C_{60}(G*n*-COOMe) at the air/water interface. The isotherms displayed liquid, solid, and collapsed phases. The occupied areas per molecule were estimated by extrapolating the linear solid phase to zero pressure. The occupied area per molecule of C_{60}(G0.5-COOMe), C_{60}(G1.5-COOMe), and C_{60}(G2.5-COOMe) is 0.62, 0.78, and 1.35 nm^2, respec-

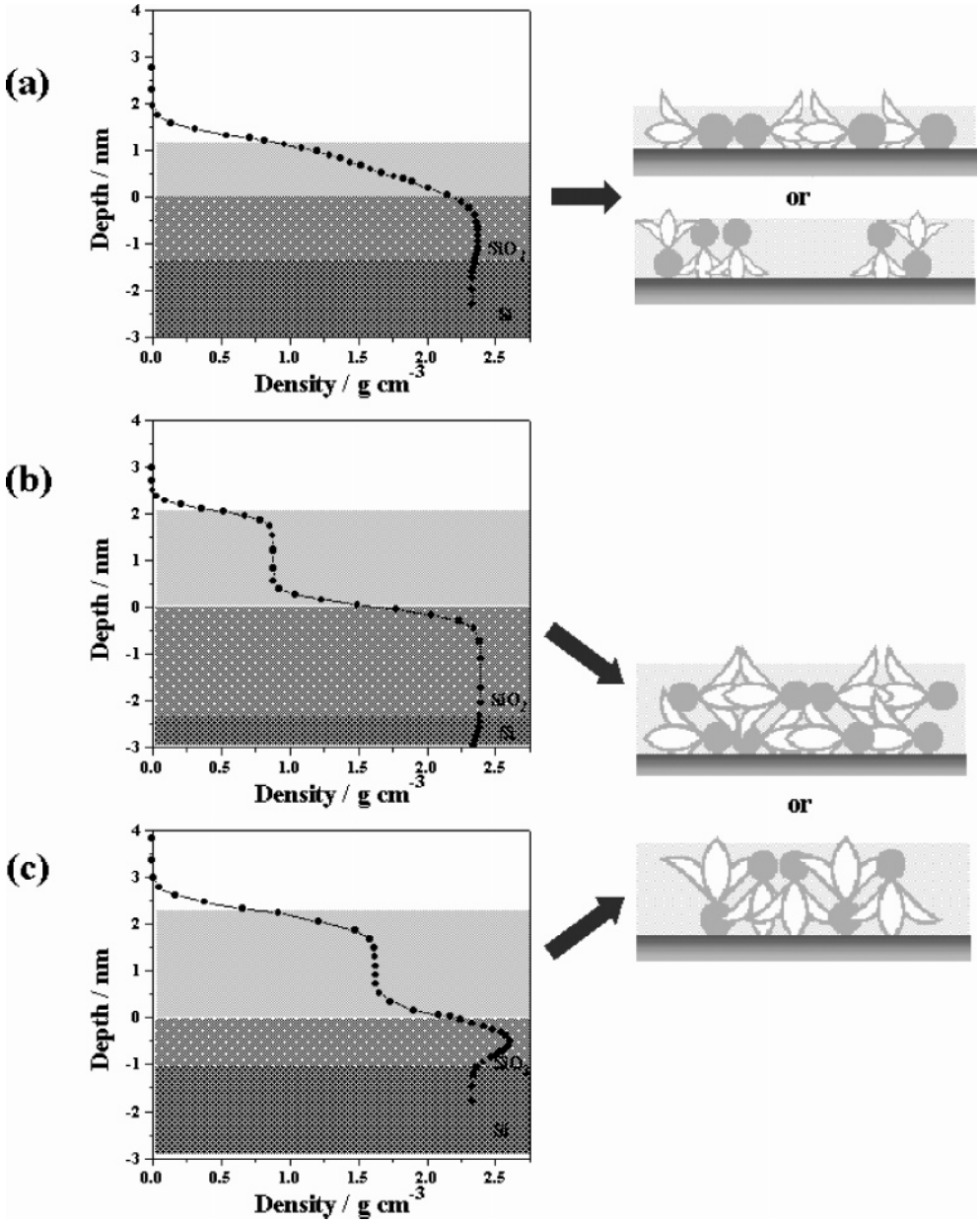

Figure 5. Depth profile of adsorption films of C_{60}(G*n*-COOMe) ($n = 0.5, 1.5, 2.5$) and schematic illustration of molecular arrangements at the air/silicon interface. (a) C_{60}(G0.5-COOMe); (b) C_{60}(G1.5-COOMe); (c) C_{60}(G2.5-COOMe).

tively. The reported limiting area of C_{60} derivatives was 1.0 nm^2.[17,18,21] In the case of C_{60}(G0.5-COOMe) and C_{60}(G1.5-COOMe), the experimental value is less than the expected value for a fullerene moiety, suggesting that molecules are either, at least, partially offset or accumulated in the Langmuir film. As for C_{60}(G2.5-COOMe), the occupied area is significantly larger than the expected one. This indicates that the bulky dendritic moiety disturbs close packing of fullerene moieties and controls the occupied area per molecule. The estimated molecular arrangements at the air/water interface are shown in Figure 2.

Molecular Arrangements in C_{60}(G*n*-COOMe) LB Films. Figure 3A shows XR curves of the LB films of C_{60}(G*n*-COOMe) on the silicon wafer. The ordinate is the reflectivity in logarithmic scale, and the abscissa is a scattering vector Q_z. In the all cases, a few fringes were produced by the reflection at the interface, indicating the existence of a layered film. However, the profiles were different among three generations of C_{60}(G*n*-COOMe). The depth/density profiles evaluated from computer simulation and the cartoons of molecular arrangement in the C_{60}(G*n*-COOMe) films are given in Figure 4.

As for C_{60}(G2.5-COOMe), using a two-layer model, the reflection curve was well reproduced with the parameters in Table 1, as seen in Figure 3A. The fitting shows that the thickness of the upper layer, 1.55 nm, is almost the same as the size (~1.3 nm) of C_{60} + anthracene. The layer of the air side was slightly denser than that of the substrate side. In addition, the density of the fullerene layer was calculated to be 1.39 and 1.2 g cm^{-3} for hexagonal and square 2D lattice packing, respectively. The lower density, 0.98 g cm^{-3}, which was evaluated for the upper layer, is reasonable as a loose fullerene packing, since the occupied surface area (1.35 nm^2) of the Langmuir film is larger than the reported value (1.0 nm^2),[17,18,21] as described above. These observations indicate that the upper layer is the fullerene moiety. For the lower layer, the density and thickness values are appropriate for the dendron moiety, because the dendron moiety is less dense than

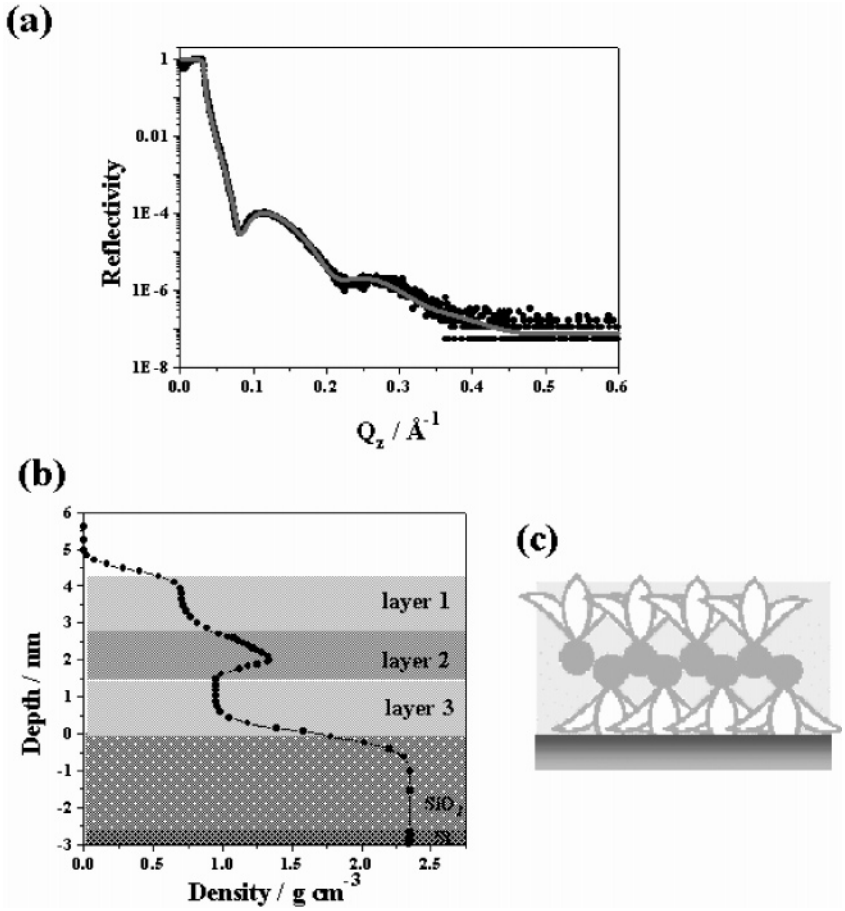

Figure 6. XR curve, depth profile, and schematic illustration of molecular arrangement of an adsorption film of C_{60}(G2.5-COOK) at the air/silicon interface. (a) XR curve (the closed circles are experimental data and solid gray line is the optimum fitting curve); (b) depth profile; (c) schematic illustration.

the fullerene moiety and has a flexible size. Thus, the LB film of C_{60}(G2.5-COOMe) is constructed of the two layers of the hydrophobic fullerene moiety (upper layer) and the hydrophilic dendron moiety (lower layer) (see Figure 4c). This indicates that C_{60}(G2.5-COOMe) has strong amphiphilic properties.

On the other hand, the results of the optimum fitting calculation for XR curves of C_{60}(G0.5-COOMe) and C_{60}(G1.5-COOMe) indicate that their LB films are constructed of four layers. The top and bottom layers of the C_{60}(G1.5-COOMe) film are less dense than the middle layers, as seen in Table 1 and Figure 4b. This fact suggests that, at the air/substrate interface, the LB film of C_{60}(G1.5-COOMe) consists of a double layer of molecules in which the fullerene moiety exists in the interior layers of the films. The lower part in the interior layers of C_{60}(G1.5-COOMe) had a higher density than the upper one, indicating that molecules in the lower layer were more dense than those in the upper one. Whereas the thickness of the dense interior layers was 2.45 nm for the C_{60}(G1.5-COOMe) film, it was only 0.82 nm for the C_{60}(G0.5-COOMe) film. Therefore, it was concluded that the C_{60}(G0.5-COOMe) film was quite unlike the simple double layer (bilayer), but the fullerene moieties in top and bottom molecules interpenetrated. The dendron moiety of the lower monolayer in the double layer of C_{60}(G0.5-COOMe) was calculated as two layers.

The size ratio of fullerene moiety to dendron or the shape of the molecule is important in molecular arrangement in the film. When the fullerene moiety is larger than the dendron moiety (see Figure 1), the fullerene−fullerene interaction acts strongly between molecules. This is a case of C_{60}(G0.5-COOMe). If the fullerodendron molecule takes a cylindrical structure as a case of C_{60}(G1.5-COOMe), the molecule prefers to make a typical double layer (bilayer) on the solid substrate due to the balance of fullerene−fullerene interaction and molecular amphiphilicity. These film structures are in contrast to that of C_{60}(G2.5-COOMe). At a higher generation of fullerodendron, the monolayer formation ability at the air/water interface as an amphiphilic molecule is stronger than the fullerene−fullerene interaction that prevents the monolayer formation.

Molecular Arrangements in C_{60}(G*n*-COOMe) and C_{60}(G*n*-COOK) Adsorption Films. Figure 3B shows XR curves for the films of C_{60}(G*n*-COOMe) adsorbed on a silicon wafer, and the density−depth profiles are shown in Figure 5. It is implied that the adsorption films consist of the mixture of fullerene and dendron moieties, since the best-fit density−depth profiles were obtained only by one layer but not by a multilayer, despite the fact that there is a difference of densities between fullerene and dendron moieties. The parameters are listed in Table 1. In the case of C_{60}(G0.5-COOMe), the layer thickness was only 0.91 nm, which is close to the diameter of fullerene. This fact indicates that the molecules adsorb with the molecular axis parallel to the substrate or the substrate is partly occupied by adsorbed molecules. The large roughness (0.55 nm) evaluated supports the latter case. On the other hand, C_{60}(G1.5-COOMe) and C_{60}(G2.5-COOMe) films were thicker than the C_{60}(G0.5-COOMe) film but still one layer, implying that the molecules adsorbed with random orientation. Possible molecular arrangements are illustrated in Figure 5.

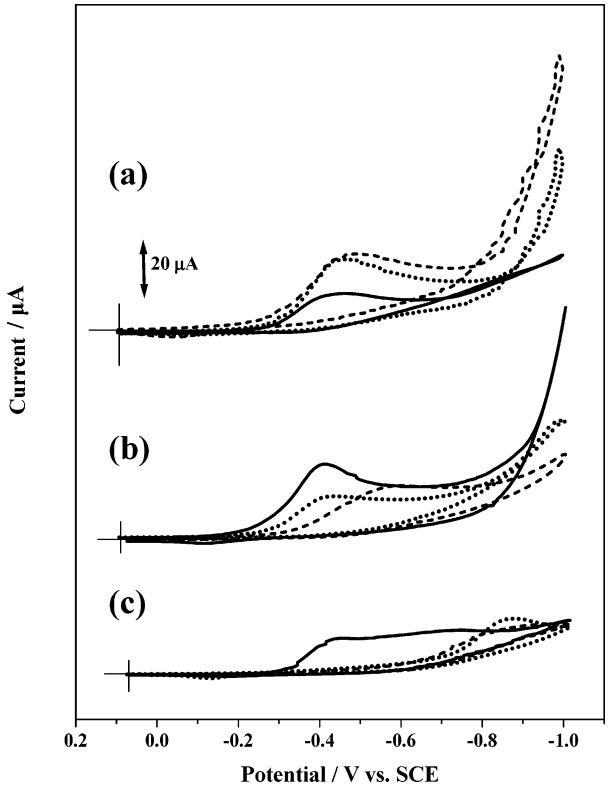

Figure 7. Cyclic voltammograms of LB films of C_{60}(Gn-COOMe) (n = 0.5, 1.5, 2.5) in an aqueous 0.5 M TBAC solution, before (solid line) and after UV light irradiation under oxygen (dashed line) and nitrogen (dotted line) flux. The sweep rate is 50 mV s^{-1}. (a) C_{60}(G0.5-COOMe); (b) C_{60}(G1.5-COOMe); (c) C_{60}(G2.5-COOMe).

Figure 6 shows a XR curve of the C_{60}(G2.5-COOK) adsorption film on the silicon wafer and its density−depth profile. Different from the C_{60}(Gn-COOMe) adsorption films, this film resembles the LB films of C_{60}(G0.5-COOMe) and C_{60}(G1.5-COOMe) in molecular arrangement, that is, it consists of three layers or a double layer of molecules (see Figure 6). An affinity of the terminal $-COO^-$ or −COOH groups of fullerodendron to the silicon wafer and the fullerene−fullerene interaction are the driving forces for the hierarchical arrangement in the adsorption film. Lower generation molecules of C_{60}(Gn-COOK) did not adsorb on the silicon wafer. They are inferior to form stable adsorption films due to fewer hydrophilic groups against the fullerene moiety.

Effect of UV Light Irradiation on Electrochemical Properties of C_{60}(Gn-COOMe) LB Films. The cyclic voltammetric measurements in an aqueous 0.5 M TBAC solution were performed with a sweep rate of 50 mV s^{-1} and are shown in Figure 7. Before light irradiation, all C_{60}(Gn-COOMe) LB films exhibit a reduction response around −0.4 V that could be attributed to the generation of radical monoanion of the fullerene moiety.[7] However, an oxidation peak could not be observed, indicating that the reduction of these films is irreversible although details are unknown at present. The high current feature close to −1.0 V may be due to the reduction from monoanion to dianion. As to both C_{60}(G0.5-COOMe) and C_{60}(G1.5-COOMe), after light irradiation, the reduction peaks around −0.4 V remained without shift under nitrogen flux and slightly shifted under oxygen flux. The shift might be caused by the oxygen doping into the fullerene film, and that makes the films harder to be reoxidated. However, irrespective of the presence of oxygen or nitrogen, UV light irradiation makes a reduction peak

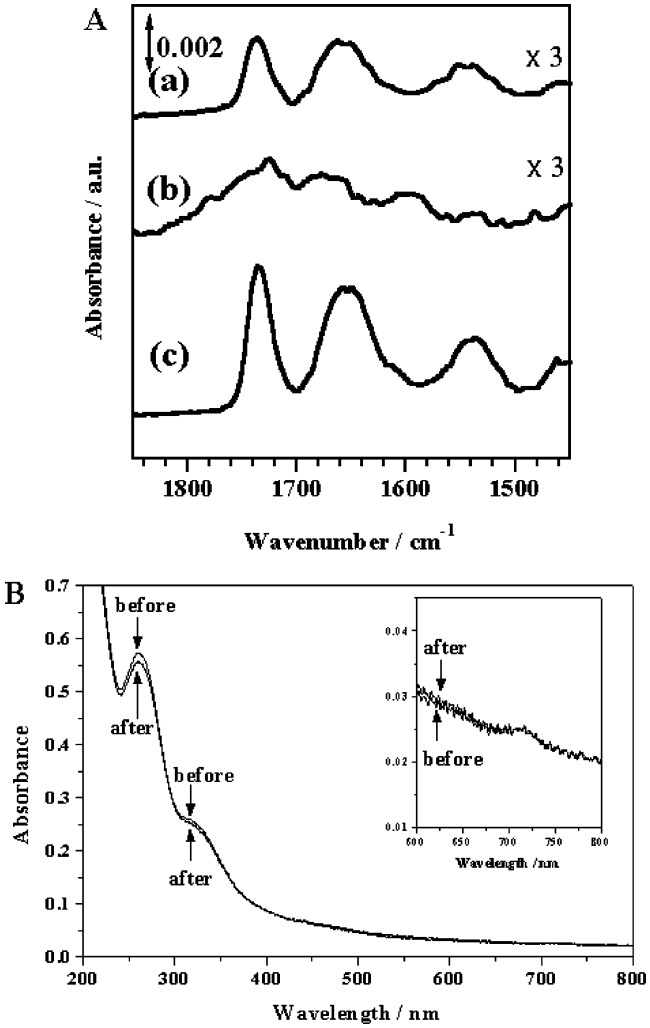

Figure 8. (A) IR-RA spectra of C_{60}(G2.5-COOMe) in the LB film (a) before and (b) after UV light irradiation. For comparison, an IR-RA spectrum of a cast film of C_{60}(G2.5-COOMe) is included as spectrum c. (B) UV−vis spectra of a cast film of C_{60}(G2.5-COOMe) on a quartz substrate before and after UV light irradiation.

of C_{60}(G2.5-COOMe) LB film disappear, and voltammograms of irradiated films were similar to that of an arachidic acid LB film (not shown in this paper).

Figure 8A shows IR-RA spectra of a C_{60}(G2.5-COOMe) LB film before and after UV light irradiation. Before irradiation, there are three main vibration bands in the 1800−1500 cm^{-1} region. The strong vibration band around 1736 cm^{-1} is due to the C=O stretching mode of terminal ester. The bands at 1658 and 1536 cm^{-1} are attributed to amide groups of the dendron moieties. After irradiation, a band at 1597 cm^{-1} assigned to the COO^- antisymmetric stretching vibration mode appeared, implying that ester groups of the dendron moiety were partially decomposed to carboxylate by the UV irradiation.

Figure 8B shows UV−visible spectra of C_{60}(G2.5-COOMe) LB films before and after UV light irradiation. The absorption bands around 260 and 715 nm are attributed to fullerene cages and anthracene adduct of fullerene, respectively. Irrespective of the UV irradiation, both spectra were similar to each other, suggesting that the fullerene cages and C_{60}−anthracene binding were not broken.

From IR and UV−visible absorption spectra, the UV light irradiation damages only dendron moieties. C_{60}(G2.5-COOMe) is vulnerable to this effect, because it

has a big dendron moiety. Moreover, the fullerene−fullerene interaction in its LB film is rather weaker than that of other generations from the viewpoint of molecular arrangement in the film, as discussed above. The variation of methyl ester moiety to carboxylate species by UV light irradiation led to the assumption that the C_{60}(G2.5-COOMe) molecule dissolved into water after UV light irradiation. Thus, the disappearance of the reduction peak of the C_{60}(G2.5-COOMe) LB film in the cyclic voltammogram is owing to the dissolving of C_{60}(G2.5-COOMe) from the LB film. There was a stark difference between generations, which is caused by the difference of molecular arrangement in the LB films. In the cases of C_{60}(G1.5-COOMe) and C_{60}(G0.5-COOMe), which form double layers in the LB films, since ester decomposition by UV light irradiation may occur at the top layer, their dissolution does not happen.

Conclusions

In this study, LB and adsorption films of the fullerodendrons have been investigated. The structural characterization was performed by X-ray reflectometry, which is a powerful tool for analyzing the interfacial structure.[28] It was revealed that dendron generations, film fabrication methods, and terminal group species make molecular arrangements in the films and electrochemical properties of the films different. The LB film formation by fullerodendrons is controlled by the competition of the fullerene−fullerene attractive interaction and monolayer formation ability of the dendron moiety. As a result, we succeeded in the preparation of a two-dimensional array of fullerene, which was sandwiched by low-generation dendron moieties or exposed on a high-generation dendron layer. Arrays of fullerodendrons in the films affected the photoelectrochemical properties. Construction of two-dimensional films of fullerene is expected to be useful in applications for sensors and devices.

Acknowledgment. This work was supported by a Grant-in-Aid for Scientific Research on Priority Areas (417) from the Ministry of Education, Culture, Sports, Science and Technology (MEXT) of the Japanese Government.

LA048161U

(28) Mitamura, K.; Takahashi, M.; Hamaguchi, S.; Imae, T.; Nakamura, T. *Trans. Mater. Res. Soc. Jpn.* **2004**, *29*, 255.